Continuous Wave Laser Gas Heating by Sustained Plasmas in Flowing Argon

H. Krier,* J. Mazumder,† T.J. Rockstroh,‡ T.D. Bender,‡ and R.J. Glumb§
University of Illinois, Urbana, Illinois

This paper reports the results of an in-depth study of laser-sustained plasmas in flowing argon for application to laser propulsion. The experiments were performed in a pressurized absorption chamber using a 10 kW CO_2 laser. Global absorption measurements have been carried out under a range of laser powers, pressures, and flow rates, indicating a total absorption approaching 80%. Thermocouples have been used to map gas temperatures in the downstream mixing zone. These mappings were used to estimate thermal conversion efficiencies. Thermal efficiency was found to be 6–25%, depending on the pressure, flow rate, and laser power. These thermal efficiencies correspond to radiative losses of 64 and 30%, respectively. Two-dimensional spectroscopic relative-intensity temperature mappings of the plasma core agree spatially with the results of a numerical model. The spectroscopic data indicate peak plasma temperatures of 18,000 K, with the global absorption of laser energy calculated to be 56.2%.

Nomenclature

A = area normal to gas flow, m^2
C_p = specific heat at constant pressure, J/kg·K
E_ℓ = energy of upper levels, eV
e = radial dependent emissivity
$\dot{h}$ = enthalpy flux, J/s
k = Boltzmann constant, J/K
$\dot{m}$ = bulk mass flow rate, kg/s
N = atomic number density, cm^{-3}
N_e = electron number density, cm^{-3}
T = radially dependent measured temperature, K
T_e = electron temperature, K
T_{exit} = bulk exit plane gas temperature, K
T_{in} = entrance working gas temperature, K
V = temperature dependent velocity of gas, m/s
ρ = temperature dependent density of gas, kg/s^3

I. Introduction

DURING the past decade, interest has steadily grown in the idea of using high-energy lasers for beamed energy propulsion applications. Such a scheme has an important potential advantage over existing propulsion systems: the ability to produce moderate levels of thrust at high specific impulse.[1,2] Laser propulsion could bridge the gap between high-thrust, low-specific-impulse chemical systems and high-specific-impulse, low-thrust electric propulsion.

In continuous wave (CW) laser propulsion, a stable laser-sustained plasma (LSP) is used to convert the remote laser energy into the thermal energy of a propellant gas. The underlying physics of the LSP must be fully explored before the feasibility of laser propulsion can be assessed. The purpose of the experiments currently being conducted is to study LSPs in flowing argon to reveal absorption behavior, temperature profiles, mixing behavior, radiative losses, and laser-to-thermal energy conversion efficiencies.

One of the first experimental studies of laser-supported plasmas for propulsion was conducted in 1974 by Pirri et al.[3] In these tests, a quasi-CW laser struck solid targets and the impulse produced was measured. One conclusion of these experiments was that a more stable method of heating the propellant was needed.

It was soon recognized that a plasma held stationary in a gas flow could be used as the source of such stable heating. Laser-sustained air plasmas have been studied by physicists for some time, especially in the Soviet Union, and a thorough experimental study of these plasmas in air was made by Fowler and Smith in 1975.[4] They found that the plasmas tended to be stable phenomena as long as the f number of the focusing optics was less than 10. Typically, the plasma would be ignited at the focus point and would then begin propagating back into the converging beam until it reached a location where the laser intensity matched the intensity required to sustain the plasma. Another finding was that roughly half the laser energy passed through the plasma without being absorbed. Fowler and Smith also used a laser interferometer to obtain accurate two-dimensional temperature and number density profiles of the stationary air plasmas. Results indicated peak temperatures of over 16,000 K.

Henricksen and Keefer[5] conducted similar experiments using spectroscopic analysis of continuum radiation. Their technique yielded peak temperatures near 17,000 K and maintenance intensities of 120 kW/cm^2 were reported.

More recently, the experimental work has been extended to hydrogen plasmas by Fowler,[6] who studied laser-sustained plasmas in hydrogen and hydrogen/seed mixtures. The focus of this work was to measure the absorption coefficient of the various mixtures as a function of temperature. The effect of adding a seedant is a dramatic increase in the absorption coefficient at low temperatures. In general, this results in a lower-temperature plasma and may lower radiative losses.

In 1979, Conrad et al.[7] were successful in creating stationary plasmas in flowing hydrogen gas. Using a 30 kW CW laser, they showed that initiation occurred at intensities an order of magnitude lower than had been predicted (experimental values near 3×10^5 W/cm^2) and that the absorption process was generally stable.

After this, Van Zandt and McCay[8] began studying hydrogen plasmas in more detail by investigating the plasma

Presented as Paper 85-1551 at the AIAA 18th Fluid Dynamics and Plasmadynamics and Lasers Conference, Cincinnati, OH, July 16-18, 1985; received July 29, 1985; revision submitted Jan. 24, 1986.

*Professor of Mechanical Engineering, Department of Mechanical and Industrial Engineering. Associate Fellow AIAA.

†Associate Professor of Mechanical Engineering, Department of Mechanical and Industrial Engineering.

‡Graduate Research Assistant, Department of Mechanical and Industrial Engineering.

§ONR Fellow, Department of Mechanical and Industrial Engineering. Student Member AIAA.

initiation process and measuring temperatures within the plasma region. Plasma initiation was produced using a 6 J, 100 ns pulsed CO_2 laser cofocused with the CW maintenance laser through the primary NaCl optics. Temperatures were measured by digitally analyzing the output of a filtered video camera and using the absolute intensity of continuum radiation to determine electron temperature.

Similar work is being done at the University of Tennessee by Keefer et al.[9] Using a 1.5 kW CO_2 CW laser focused into a small-diameter quartz tube, Keefer is studying the absorption processes in the core region of argon plasmas. A small-diameter chamber is used so that the convective flow in the core can be closely observed. Temperature data are obtained by measuring the absolute intensity of continuum radiation from the plasma, using digital image acquisition and processing.

This paper presents the results of ongoing experiments designed to fully characterize laser-sustained plasmas in flowing argon. The goals of the research are to 1) spectroscopically measure the temperatures within the plasma core using line-to-continuum techniques, 2) measure the global laser energy absorption of the LSP under various flow conditions, and 3) produce detailed thermocouple mappings of the downstream flow region and use these to estimate thermal conversion efficiencies and radiative losses. Argon has been used as the test gas due to its well-documented properties and for safety considerations. Also, the absorption and emission behavior of argon is similar to that of hydrogen. Hydrogen is the propellant of choice due to its low molecular weight.

II. Experimental Apparatus

The laser employed in the experiments is an Avco-Everett, model HPL 10, CW CO_2 laser capable of sustained 10 kW beam output at 10.6 μm. The laser is an unstable oscillator and the expanded output beam resembles a TEM^*_{01} mode structure, which is annular with a near-Gaussian energy distribution over the annulus. To facilitate materials processing (the laser's primary function), the annular beam has an expanded diameter of 2.6 in.

Laser-sustained plasmas are created by focusing the laser inside a cylindrical absorption/flow chamber shown in Fig. 1. The chamber is placed vertically at the test stand to preserve the internal axial flow symmetry in the presence of strong buoyancy effects. The chamber, attachment flanges, and window assemblies were machined from 304 stainless steel, chosen for its strength and corrosion resistance. A 5 in. i.d. was selected to minimize wall interference effects when studying mixing in the downstream flowfield.

To focus the horizontal laser beam up and into the chamber, the laser optics layout shown in Fig. 2 was devised. The beam is directed by two 5.0 in. copper flat mirrors into a 4.5 in. convex copper mirror, which spreads the beam and directs it down into a 20.0 in. concave mirror located directly below the chamber. The beam is then focused up through a 6 in. salt window to a specific point inside the chamber.

The advantage to using this rather complex optical system is that by changing the relative distances between the convex and concave mirrors, the f number of the converging beam can be varied between 2.2–3.4. This allows examiantion of the stability, shape, initiation, and absorption characteristics of the plasma under a variety of beam geometries. The energy flux through the salt window is also minimized by expanding the beam at the chamber inlet. The best estimate of the $1/e$ spot size is 0.8 mm, utilizing a HeNe alignment laser. This off-axis optical system introduces astigmatism and coma into the focal volume and experiments are underway to map the infrared focal volume.

Both NaCl and KCl salt window blanks are used interchangeably in the laser window assembly. For the higher-pressure tests up to 5 atm absolute, 1.35 in. thick Polytran NaCl windows are used. The NaCl blanks were found to progressively crack during prolonged use. This was caused by thermal stresses produced by fractional absorption of the laser beam. The Polytran windows are more resistant to failure and tend to craze instead of fracture when stressed. The windows also have a tendency to fog when exposed to humidity in the air. The fogging, unless severe, was determined to have no appreciable effect on the transmittance.

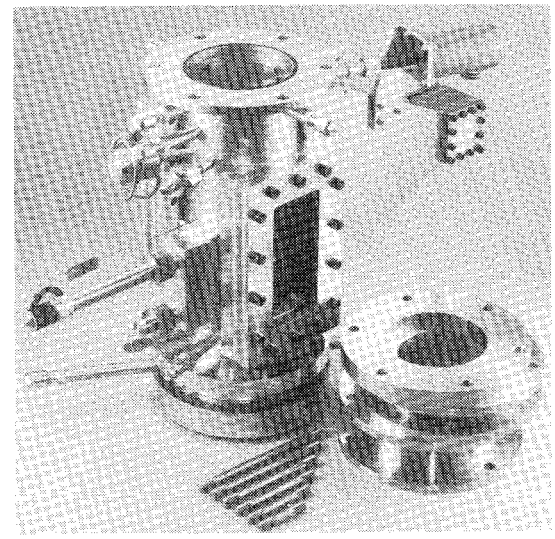

Fig. 1 Stainless steel plasma absorption/flow chamber.

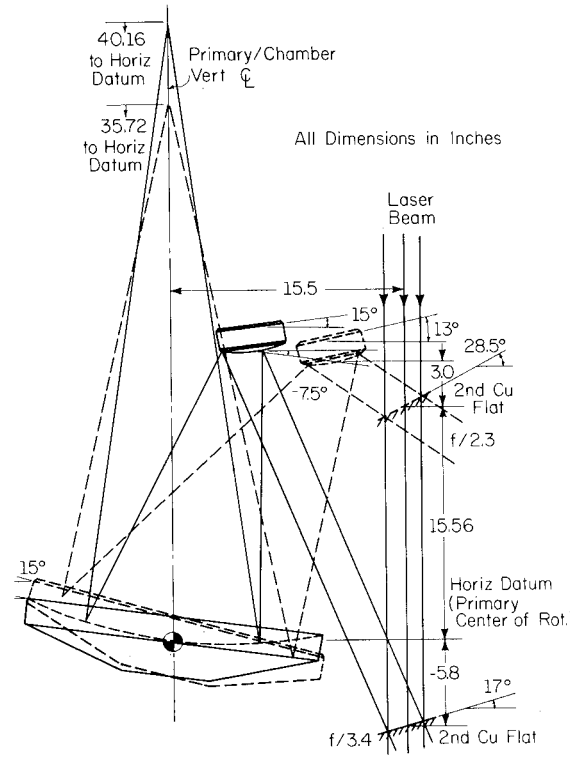

Fig. 2 Mirror positions at design limits.

Pressurized gas is injected into the chamber through the gas inlet assembly shown on the bottom of the chamber in Fig. 1. Gas flows into the chamber directed by a group of small holes drilled in the inner annular ring of the assembly. The current hole arrangement directs a portion of the incoming flow back onto the laser inlet window for cooling purposes.

The gas handling system used with the chamber is designed to produce steady internal flow at pressures up to 5 atm. Gas exiting the chamber is passed through a water-cooled heat exchanger to prevent downstream valve damage. The argon mass flow rate is controlled by a valve downstream from the

heat exchanger. Through adjustment of the gas tank regulators and the downstream valve, any combination of chamber pressure and flow rate can be selected. The bulk exit temperature depends on the laser power used, the mass flow rate, the absorption efficiency, the type of gas used, and the beam geometry. The flow rates used in the experiments were 2.3–4.6 g/s of argon, corresponding to bulk flow velocities of 11–22 cm/s.

To measure the fraction of incident laser power transmitted through the plasma, an Avco-Everett high-flux calorimeter is used as a beam dump. The water-cooled copper cone of the calorimeter is bolted to the top of the chamber shown in Fig. 1. The calorimeter instrumentation measures the change in water temperature with two arrays of thermocouples. The analog voltage difference between these two arrays is used to calculate the power collected. Once the transmitted power is known, the fractional absorption is found by assuming that all of the incident laser power that was not transmitted was absorbed by the plasma.

To produce plasma initiation, either the laser energy flux at the focus must be of sufficient magnitude to initiate breakdown or free electrons must be introduced artificially into the gas at the focus. Since the laser optical system and the available laser power are inadequate to produce breakdown by the first method, free electrons are supplied artificially by vaporizing zinc foils at the laser beam focus. Zinc and other low vaporization temperature metals are good absorbers of 10.6 μm radiation. Electrons freed during vaporization start the electron cascade, which results in ionization of the gas.

The foil initiation system has proved very reliable. Plasma initiation proposals involving the injection of particles or aerosols at the focus are still under study. Initiation using aerosols has been found to be possible but unreliable.

A FLUKE model 2452 MCS (measurement and control system) is used to remotely sequence, monitor, and control aspects of the experiments. Part of the monitor function is the collection and storage of data. Data stored using the FLUKE includes chamber pressure, chamber temperature, thermocouple carriage temperatures, exit gas temperature, calorimeter output, and other temperature measurements used in safety monitoring. The system is also used to operate the stepper motors used to position the diagnostic equipment.

III. Thermocouple Diagnostics

The laser power incident at the plasma will be fractionally absorbed and then either retained by the gas or reradiated to the chamber walls. These fractions must be measured, since determining the thermal conversion efficiency of a laser propulsion system as a function of laser power, beam geometry, gas pressure, and flow velocity is a principal aim of laser propulsion research.

Gas temperatures under 3000 K in the flow around the plasma are measured with tungsten-rhenium thermocouples.

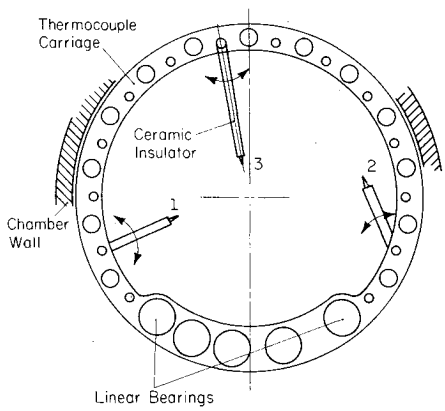

Fig. 3 Thermocouples mounted on moveable carriage (thermocouples can be pivoted for a variety of scan configurations).

These thermocouples are mounted on a movable carriage capable of traversing the chamber length. Figure 3 shows an axial view of the carriage and three thermocouple orientations. A remotely programmed stepper motor moves the carriage through the downstream flow region. This allows us to construct two-dimensional temperature mappings of the flow around the plasma.

Figure 4 is a scale view showing the region in which the thermocouple measurements are made. The exhaust plane of the chamber is considered the rightmost edge of the measurement zone, downstream from the plasma. Notice that the laser beam intersects part of the measurement zone in this example. Corrections for direct radiative heating of the carriage thermocouples by the laser beam have been included in the results. The plasma core is too hot to measure with thermocouples, so it is avoided. The thermocouples are found to reach their temperature limits at a distance of 5–6 mm from the centerline. This upper limit to plasma size is in agreement with the spectroscopic surveys discussed in Sec. V.

Figures 5–7 are two-dimensional temperature mappings of the measurement zone seen in Fig. 4. The isotherms are constructed from a grid of discreet measurement points spread evenly through the measurement zone. The temperatures along the wall are around 400 K and near the plasma as high as 2600 K.

The isotherms indicate the shape of the mixing layer around the plasma and the shape of the hot buoyant plume downstream. The temperature gradients upstream of the

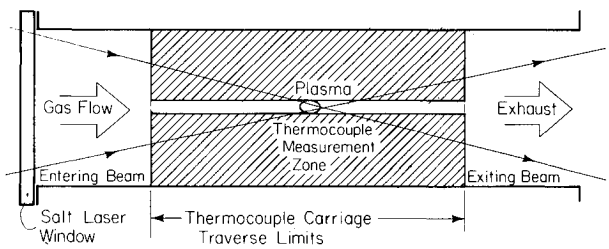

Fig. 4 Area in which thermocouple measurements have been made.

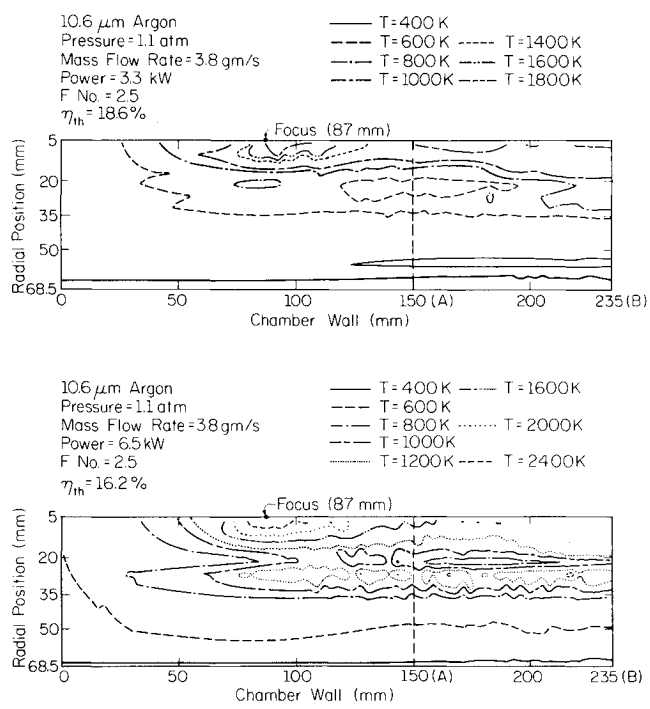

Fig. 5 Two-dimensional temperature mappings under low mass flow rate, low pressure, and two incident laser powers (estimated thermal efficiencies are also listed).

plasma as measured by the thermocouples are not as steep as expected. This may be due to radiative heating of the thermocouples by the plasma. Direct radiative heating of the thermocouples by the transmitted laser beam when measuring portions of the downstream flow is found to be small. This increases confidence in the viability of making exit enthalpy calculations based on temperatures recorded in this area.

The temperature mappings of Fig. 5 are for low pressure, low mass flow rate, and two laser powers. A comparison of Figs. 5a and 5b shows that increasing the laser power increases the size of the plasma, the temperatures near the plasma core, and the downstream exit plane temperature. The plasma is also seen to be located upstream of the laser beam focus, as predicted by analytical models.

Figure 6 shows two temperature mappings made at low pressure, high mass flow rate, and two laser powers. Again, an increase in laser power is accompanied by an increase in plasma size and a slight increase in temperatures near the core and in the downstream mixing region. In addition, the increased flow rate lowers the bulk temperatures near the exit.

Figure 7 shows two mappings at high pressure, low mass flow rate, and two laser powers. The same trends as before are apparent with increased laser power. Also, the increase in pressure seems to cause the plasma to become hotter and to reduce the downstream temperatures.

For each temperature mapping, the fraction of the incident laser power retained by the gas as thermal energy is estimated by calculating the enthalpy flux at the exit plane. The gas enthalpy flux is calculated using an average exit temperature calculated from a mixing cup analysis that incorporates velocity. This mixing cup temperature is given by

$$\bar{T}_{\text{exit}} = \frac{1}{\dot{m}} \int \rho V T \, dA \tag{1}$$

The change in enthalpy flux is then given by

$$\Delta \dot{h} = \dot{m} C_p (\bar{T}_{\text{exit}} - T_{\text{in}}) \tag{2}$$

Equation (1) is integrated over the exit plane using the temperatures from the thermocouple mappings. The thermal efficiency is then the ratio of the change in enthalpy flux to the input laser power.

Because the velocity fields in and near the plasma are unknown, it has been assumed that ρV is a constant, allowing a much simpler integration of Eq. (1). This is essentially an assumption that the radial velocity components in the flowfield are negligible. Although we believe this to be reasonably valid at the flow velocities studied, measurements of flowfield velocities are needed to verify this.

There is also some question about the possibility of flow recirculation around the plasma due to the strong buoyancy effects present. A strong recirculation could challenge the assumption of $\rho V = \text{const}$ used in the efficiency calculations. Although this question is still under study, none of the thermocouple mappings in Figs. 5-7 show evidence of flow recirculation. The most probable velocity profile is shown schematically in Fig. 8.

Figures 5-7 list the calculated mass-averaged bulk temperatures and the corresponding thermal efficiencies. For example, under the experimental conditions listed in Fig. 5a, the fraction of the laser power incident at the plasma retained by the gas is 18.6%. And, the fact that 40% of the incident power is found from the calorimeter data to be transmitted implies that 41.4% of the incident laser power is lost to the walls in the form of radiation.

Figures 5-7 indicate that the thermal efficiency decreases with increased laser power. At the higher flow rate, the thermal efficiency is considerably greater and the radiative losses appear to be reduced. At higher pressure, the thermal efficiency is much lower, indicating that the radiation losses have increased.

Preliminary estimates of the relative magnitude of fractional plasma radiative losses have also been made by monitoring the rate of change in the chamber wall temperature. These temperatures indicate that the fraction of the incident power lost to the walls (at a constant mass flow rate and laser power) as radiation increases with increased pressure. This is consistent with the visual observation that the

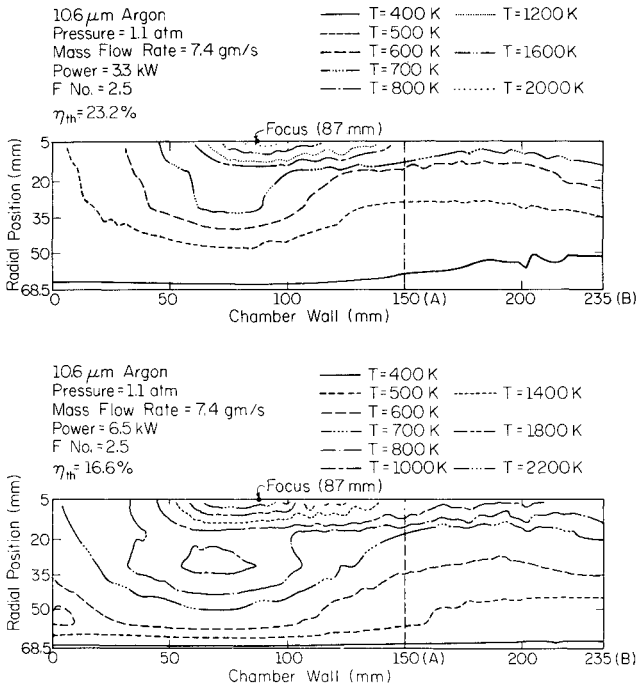

Fig. 6 Two-dimensional temperature mappings with estimated thermal efficiencies under high mass flow rate, low pressure, and two incident laser powers.

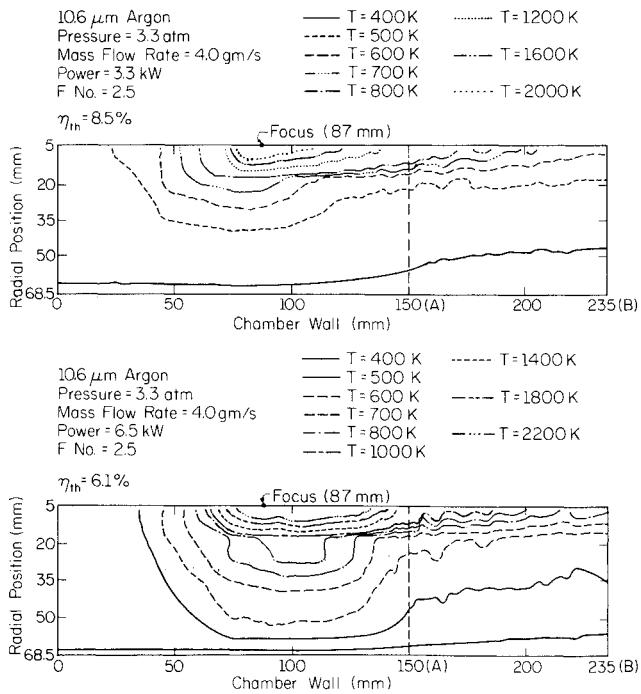

Fig. 7 Two-dimensional temperature mappings with estimated thermal efficiencies under low mass flow rate, high pressure, and two incident laser powers.

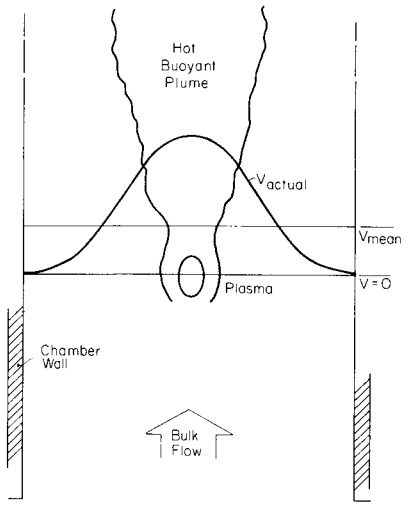

Fig. 8 Probable velocity profile based on thermocouple data.

plasma appears much brighter at higher pressure. Increasing the mass flow rate is not found to change the radiative losses substantially, although this is not surprising given the limited range of the flow velocities studied. These preliminary estimates also confirm that the fractional plasma reradiation increases with laser power.

These results represent the first experimental estimates of the thermal efficiency of a laser-sustained plasma. Although the values are preliminary, the trends are all consistent with the results of analytical modeling.

IV. Calorimeter Measurements

Measurements of global plasma absorption were made using a copper cone calorimeter attached to the top of the absorption chamber. The calorimeter measures the total power transmitted or scattered by the plasma. Scattering (reflection) can be shown to be less than 2% at the electron number densities ($< 10^{17}$ cm^{-3}) found in these plasmas. The remainder of the incident laser energy is, therefore, assumed to be absorbed by the plasma.

The global absorption measurements are presented in Fig. 9 for two different focus spot sizes at a pressure of 1.1 atm and a mass flow rate of 2.3 g/s. Data for air are also shown for comparison. The data indicate strong laser energy absorption by argon, approaching 80% at higher laser powers.

The data also show a tendency for global absorption to rise with laser power, a largely geometric effect. As laser power increases, the plasma size and therefore the absorption length grow, causing a net increase in global absorption. The data also suggest asymptotic behavior at high power. This can be explained physically. As the laser power increases, the plasma grows until it reaches a point where increasing radiative losses from the enlarged surface area offset any increases in power, preventing further growth in the absorption length. The upper absorption limit should depend largely on the beam geometry and radiative behavior.

A comparison between two focus spot sizes (minimum beam diameters of 0.8 and 2.0 mm) was also made. A smaller focal volume increases the energy density and plasma temperature at the focus, resulting in higher absorption. The effect is most noticeable at low powers.

Minimum maintenance powers for the two focus spot sizes are also shown in Fig. 9, indicating that the smaller focus will maintain a plasma at lower laser powers. This is because the plasma extinguishes when the laser intensity at the focus falls below a minimum value and a tighter focus produces higher intensities for a given laser power. We estimate the minimum maintenance intensity to be $1.0\text{–}3.0 \times 10^5$ W/cm^2.

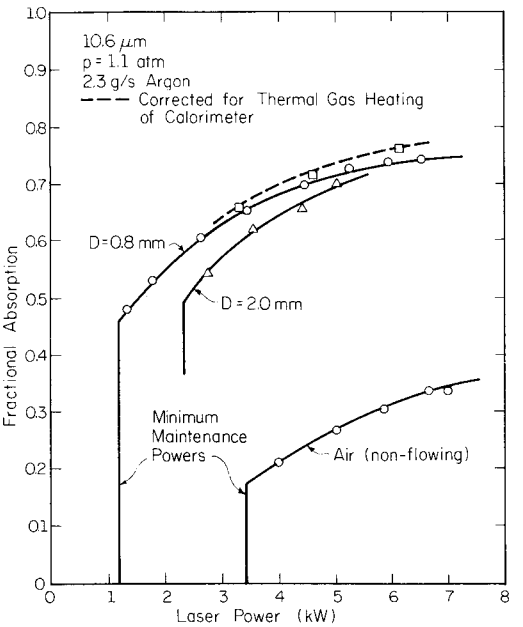

Fig. 9 Measurements of global energy absorption vs power for plasmas in argon and air (the dashed line is an analytical correction for hot gas that stagnates inside the calorimeter).

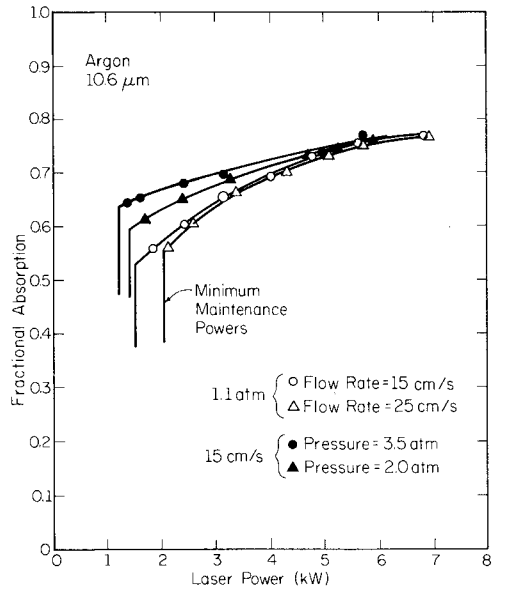

Fig. 10 Measurements of global energy absorption at higher pressures and flow rates.

The dashed line above one set of argon data represents a correction factor for heated gas that stagnates in the calorimeter cone and causes an increase in heat transfer to the cone. The correction factor is calculated using thermocouple readings from inside the cone in conjunction with analytical boundary-layer correlations. The correction becomes significant only at the higher laser powers. The thermal heating of the calorimeter will eventually be measured directly by placing a salt window between the hot plume and the calorimeter and repeating the absorption measurements.

Absorption data for air (natural convection) is presented in Fig. 9 for comparison. The air data appear to be considerably lower than argon, which is unexpected due to the similarity of the thermal properties and absorption coefficients of air (nitrogen) and argon. The air, being a molecular gas, transfers a larger amount of energy from the electrons to the heavy particles due to the larger collisional cross section and elastic and

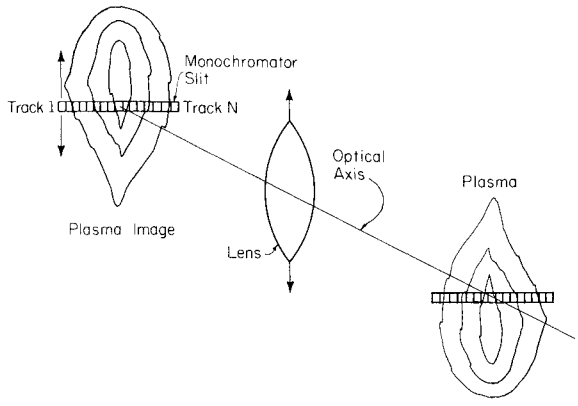

Fig. 11 Optical system utilized in spectroscopic (OMA) diagnostics.

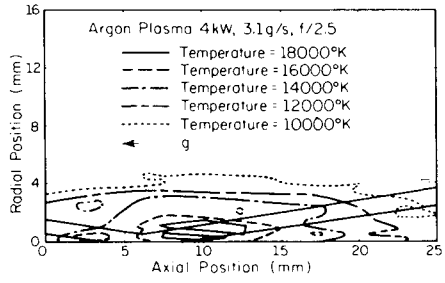

Fig. 12 Spectroscopic temperature mapping of plasma core.

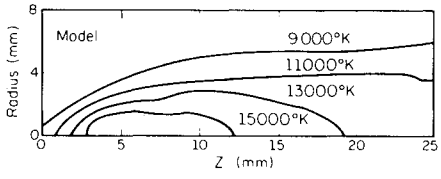

Fig. 13 Result of numerical model[12] for conditions shown in Fig. 12.

inelastic energy transport. In particular, the vibrational levels of nitrogen can store a significant amount of energy that may subsequently be transferred to the calorimeter walls, biasing the transmitted energy measurement. Thus, the absorption in air could actually be closer to the argon data. Alternately, due to the steep temperature gradients near the plasma core, the recombination effects in air may be depleting the electron population, thus reducing the absorption coefficient.

Figure 10 presents additional data taken at higher pressures and higher mass flow rates. The effect of increasing the gas pressure is to raise the absorption at low laser power and to lower the minimum power needed to sustain the plasma. However, there does not appear to be any significant difference in absorption as the laser power is increased past about 5 kW.

The effect of increasing the flow rate is less obvious. There appears to be a slight drop in absorption, but the difference is within the experimental uncertainty of the data, so no definite conclusion can be drawn. However, the difference in minimum maintenance power is clear, indicating that the plasma is less easily maintained at the higher flow rate. Both of these observations concur with ongoing modeling work, which predicts a slight lowering of global absorption with increasing flow rate, as well as a slightly higher minimum maintenance power.

V. Spectroscopic Diagnostics

Description of Technique

The relatively high temperatures (9000–18,000 K) encountered in the plasma core render conventional temperature diagnostics impractical. Spectral diagnostics based on the assumption of local thermodynamic equilibrium are the primary tool used in this temperature range. Several spectroscopic techniques are applicable and fall into two general categories, absolute and relative.

In this study, we have opted to perform relative diagnostics because the electron temperature can be calculated from emission data without the need for a calibration source. Several authors have used relative line intensity techniques to determine the temperature in arc plasmas with reasonable results.[10,11] However, when applied to argon, relative line techniques require the presence of a resolvable ArII spectra in order to determine the temperature accurately. To date, this investigation has been unable to adequately resolve the ArII spectra and has instead used the relative line-to-continuum technique at the 415.8 nm ArI metastable line.

Using the Kramer-Unsold continuum theory and quantum line radiation theory at 415.8 nm yields

$$\frac{e_\lambda(r)}{e_{C\lambda}(r)} = 1.3357\times 10^{13}\left(\frac{NT_e^{1/2}}{N_e^2}\right)\exp\left(\frac{-E_\ell}{kT_e}\right)$$

where $e(r)$ is the radial point emissivity, N the atomic number density, N_e the electron number density, E_ℓ the upper level line energy, and kT_e the electron energy. Experiments are underway to determine the error due to self-absorption, using a tunable dye laser.

Experimental Results

The spectroscopic system is an EG&G PARC optical multichannel analyzer (OMA III) with a two-dimensional vidicon detector. As shown in Fig. 11, the plasma is imaged onto the entrance slit of a 0.33 m monochromator, which spectrally spreads the incoming light across the face of a two-dimensional detector. The detector is programmed to scan N individual tracks, effectively dividing the entrance slit and hence the plasma band into N discrete elements. The element size is determined by the number of tracks, slit width, and optical magnification. Thus, each position of the slit and optics yields information for one band of plasma elements transverse to the plasma axis. The slit/optical system is then translated parallel to the plasma axis in order to map the two-dimensional intensity distribution.

The measured intensity is an integrated line-of-sight value. In order to accurately determine elemental temperatures, the integrated intensities must be converted to point emissivities via the Abel inversion. The Abel inversion is a mathematical technique that deconvolutes a cylindrically symmetrical integrated signal into the associated radial band signals. The spectral intensity mapping for the line and continuum radiation in a given plasma band is curve fit and subsequently integrated and differentiated over the line-of-sight path. This yields the emissivity as a function of radial position. The ratio of the line to continuum emissivities are then used to calculate electron temperature as discussed previously.

Figure 12 is a two-dimensional temperature mapping of the plasma core at 4 kW, 1.1 atm, 15 cm/s, and $f/2.5$. The results appear reasonable based on the results of other investigators and the lack of the ArII spectra. The discontinuities in the data are due to resolution problems in the plotting software. The straight lines are the approximate $1/e$ loci of the annular laser beam. The peak temperatures exceed 18,000 K, but may be reduced slightly based on the results of the self-absorption experiments. The error for each point has been calculated to be less than $\pm 15\%$, assuming a 10% measurement error and accounting for errors associated with the relative line-to-continuum technique. Note the off-axis peaks in temperature that correspond to the annular beam path.

Figure 13 is the result of a numerical model[12] for the same conditions as shown in Fig. 12. It can be seen that the spatial agreement is reasonable. The global absorption has been calculated for both the data and model. In the data, the incident $f/2.5$ beam is broken into 20 rays, each weighted relative to a Gaussian annular intensity profile. Point-by-point attenuation is calculated for each ray and the exiting ray bundle is summed, yielding transmitted power. The calculated absorption for the experimental data of Fig. 12 is 56.2%. The result agrees ($\pm 15\%$) with the model result of 66% and the experimental calorimeter results of 64% (Fig. 9).

VI. Conclusions

The results of an in-depth study of laser-sustained plasmas in pressurized flowing argon have been presented, including the first published mappings of the low-temperature (<3000 K) fields surrounding the plasmas. It was found that plasma initiation was easily accomplished and that plasma stability was not a problem.

Calorimetric measurements of the global laser energy absorption by the plasma indicated strong coupling of the laser energy to the gas, approaching 80% at higher laser powers. The dependence of global absorption on flow rate, beam geometry, and gas pressure were also explored. Minimum maintenance powers for a variety of flow conditions were measured.

Thermocouple mappings of the downstream flowfield indicated that the high temperatures of the plasma core are confined to a very small volume, consistent with the size measured spectroscopically. Bulk gas exhaust temperatures were found to be in the range of 400–720 K for the flow conditions presented. Thermocouple mappings were used to calculate the thermal conversion efficiencies, which were found to be 6–25%. The corresponding radiative losses were 64 and 30%, respectively. Efficiency was found to increase with flow rate, but to decrease with increased laser power or gas pressure. Preliminary measurements of radiative losses to the chamber walls suggested that the radiative losses increase substantially at higher pressures.

Two-dimensional spectroscopic temperature mappings of the plasma core region using the relative line-to-continuum technique showed electron temperatures of 9000–18,000 K. The global absorption calculated from the two-dimensional temperature field supported the experimental calorimeter measurements and the results of a numerical model.[12]

Acknowledgments

This work is funded by the U.S. Air Force Office of Scientific Research under Grant AFOSR 83-0041. Program Managers are Dr. Leonard H. Caveny and Dr. Robert Vondra. This work would not be possible without the engineering and technical services of Jon Culton and Tom Casale of the MERL 10 kW laser facility.

References

[1]Caveny, L.H. (ed.), *Orbit-Raising and Maneuvering Propulsion: Research Status and Needs,* Vol. 89, AIAA, New York, 1984.

[2]Glumb, R.J. and Krier, H., "Concepts and Status of Laser-Supported Rocket Propulsion," *Journal of Spacecraft and Rockets,* Vol. 21, Jan. 1984, pp. 70-79.

[3]Pirri, A.N., Monsler, J.J., and Nebolsine, P.E., "Propulsion by Absorption of Laser Radiation," *AIAA Journal,* Vol. 12, Sept. 1974, pp. 1254-1261.

[4]Fowler, M.C. and Smith, D.C., "Ignition and Maintenance of Subsonic Plasma Waves in Air by CW CO_2 Laser Radiation," *Journal of Applied Physics,* Vol. 46, Jan. 1975, pp. 138-150.

[5]Henricksen, B.B. and Keefer, D.R., "Experimental Study of a Stationary Laser-Sustained Air Plasma," *Journal of Applied Physics,* Vol. 46, March 1975, pp. 1080-1083.

[6]Fowler, M.C., "Measured Molecular Absorptivities for a Laser Thruster," *AIAA Journal,* Vol. 19, Aug. 1981, pp. 1009-1014.

[7]Conrad, R.W., Roy, E.L., Pyles, C.E., and Mangum, D.W., "Laser-Supported Combustion Wave Ignition in Hydrogen," U.S. Army Missile Command Tech. Rept. Rh-80-1, 1979.

[8]Van Zandt, D.M. and McCay, T.D., "Experimental Study of Laser Sparks in Hydrogen," AIAA Paper 83-1443, June 1983.

[9]Keefer, D., Crowder, H., and Peters, C., "Laser-Sustained Argon Plasmas in a Forced Convection Flow," AIAA Paper 85-0388, Jan. 1985.

[10]Key, J.F., Chan, J.W., and McIlwain, M.E., "Process Parameter Influence on Arc Temperature Distribution," *Welding Journal,* Vol. 62, 1983, pp. 1795-1845.

[11]Mills, G.S., "Emission Spectroscopy in Welding Arc Analysis," *Welding Journal,* Vol. 56, 1977, pp. 93S-96S.

[12]Glumb, R.J. and Krier, H., "A Two-Dimensional Model of Laser-Sustained Plasmas in Axisymmetric Flowfields," AIAA Paper 85-1553, July 1985.